Appl Magn Reson (2016) 47:555–565
DOI 10.1007/s00723-016-0779-3

Applied
Magnetic Resonance

EPR Detection of Iron Storage in Rat Tissues After Simulated Microgravity Model

S. V. Yurtaeva[1] · V. N. Efimov[2] · G. G. Yafarova[1,2] · A. A. Eremeev[2] · V. S. Iyudin[1] · A. A. Rodionov[3] · Kh. L. Gainutdinov[1,2] · I. V. Yatsyk[1]

Received: 14 February 2016 / Published online: 6 May 2016

Abstract By a method of spectroscopy of electron paramagnetic resonance the tissues of rats after exposure of microgravity simulation (model of hindlimb unloading) were investigated. In the tissues of heart, lung, liver and muscles the signals of electron magnetic resonance (EMR) depending on orientation were detected. The temperature and orientation dependences of the signals were studied. Comprehensive analysis of the characteristics of the EMR signals made it possible to identify the source of the signals as a crystalline magnetite. Three types of anisotropic EMR signals corresponding to a variety of spatial forms of accumulation of biogenic magnetite were detected. The appearance of the signals after microgravity simulation indicates an alteration in iron metabolism and an abnormal accumulation of iron in the rat tissues.

1 Introduction

The gravitational field is one of the inevitable environmental factors for living organisms under Earth conditions. Limitation of the effect of gravity leads to a number of systemic changes in the organisms of mammals and humans, such as body fluids redistribution; alterations in the locomotor system (muscle atrophy and decreased bone strength as a result of the calcium loss), and hematopoietic system (anemic syndrome); in the cardiovascular system (vegetative-vascular dystonia, myocardiodystrophy, atherosclerosis), and others [1]. However, the relationship

✉ S. V. Yurtaeva
yurtaeva@mail.knc.ru

[1] E.K.Zavoisky Physical-Technical Institute, The Kazan Scientific Center, The Russian Academy of Sciences, Sibirsky Trakt 10/7, Kazan 420029, Russia

[2] Institute of Fundamental Medicine and Biology, Kazan Federal University, Kremlevskaya st. 18, Kazan 420008, Russia

[3] Institute of Physics, Kazan Federal University, Kremlevskayast. 18, Kazan 420008, Russia

between the systemic, cellular and molecular mechanisms involved in the development of microgravity effects on physiology remains poorly studied.

Iron metabolism undoubtedly plays a significant role in above-listed processes. Iron metabolism incorporates the synthesis and subsequent desintegration of a number of proteins participating in functioning of the intracellular elements, such as cytochromes in mitochondria, guanylatecyclase, and other heme-containing proteins, for instance myoglobin, involved in oxygen supply system of muscle cells. Nutrient supply of iron into the body under microgravity remains as previous, under the Earth conditions, but at the same time, there is an atrophy of muscle cells and washout of the intracellular proteins and other elements, including iron-containing ones out of them. So the question arises, "Where may the iron be accumulated?"

To study the effects of microgravity under Earth conditions a rodent model of hindlimb unloading (HU) or antiorthostatic hypokinesia, based on deprivation of weightbearing by the hindlimbs, is widely used [2, 3]. HU allows to simulate on rats some physiological effects of staying in weightlessness for a long period of time; in particular—the body fluids shift to the cranial direction, which is weightlessness associated [4], the development of muscle atrophy of the hind limbs [5]. Furthermore, it is known that the HU reduces the rate of myofibrillar protein synthesis even after short period of model using [6].

The HU rat model has been accepted by scientific community as the model of choice for simulating space flight. It was established [4] that it is an adequate model to assess the hemodynamic changes in mammals, similar to those in real space flight. This model is most applicable for the cardiovascular and motor systems.

Previously the parameters of iron exchange were investigated also in humans, within the framework of the model of antiorthostatic hypokinesia, connected with bed rest in antiorthostatic position with head-down tilt of 6° [7]. A relation between changes in the body's need for oxygen and iron metabolism in conditions of antiorthostatic hypokinesia was established. That is a manifestation of the pathophysiological processes in the body in response to extreme conditions simulating weightlessness. A study of physiological changes of iron metabolism in microgravity is of interest for space medicine. The investigation on molecular mechanisms underlying the regulation of iron metabolism in microgravity may be useful for the development of approaches to prevent systemic disturbances in the conditions of space flight.

It is known that some biological processes accompanied by disturbances of iron metabolism, may course the accumulation of iron in tissues in the form of a nanosized crystalline iron oxides, as a result of biomineralization process [8, 9] in organism. Such nanoparticles may be detected by EPR spectroscopy as isotropic [10] or anisotropic [11] signals of electron magnetic resonance (EMR). These signals are characterized as the signals of EMR because they are due not to magnetic moment of isolated ion, as it is for the EPR signal but to the total magnetic moment of the crystalline particles.

The most widespread forms of nanocrystalline iron oxides in living organisms are ferrihydrite—$5Fe_2O_3{\cdot}9H_2O$ in a crystalline core of ferritin protein and magnetite—Fe_3O_4; they play a significant role in the functioning of living systems, in the

development of pathologies and may be involved in the adaptation mechanisms. The presence of such kind of particles leads to the appearance of the magnetic properties in biological tissues, and to the emergence of EMR signals.

Nowadays the EPR spectroscopy technique is widely used to determine the magnetic properties of individual paramagnetic centers or their ensembles in physical and chemical research. This method is also widely used in modern biophysical, biochemical and biomedical research, as it provides entirely new information about the molecular processes.

The aim of this study was to detect the iron oxides in the tissues of rats exposed to model simulating weightlessness by hindlimb unloading with the method of ESR spectroscopy, to determine the EMR signal parameters, and to establish their origin.

2 Materials and Methods

The study was conducted on seven laboratory rats weighting 130–150 g. Control group of three rats was also used. For microgravity simulation, we used the Morey–Holton model of HU, which is widely used for studying the effects of microgravity on the Earth (suspending animals by the tail in antiorthostatic head-down position avoiding weightbearing by the hindlimbs) [3]. After 7 days rat tissues were taken from anesthetized animals. Immediately after removal, the tissue samples were frozen in liquid nitrogen (77 K). The samples were freezing without magnetic field and stored in a frozen state before the measurements.

The crystalline forms of iron in rat tissues were studied by EPR spectroscopy technique. EPR measurements were performed on X-band EPR spectrometers—Bruker EMX and Bruker-ESR-300 at a temperature of liquid nitrogen (77 K), and in the range of 7–260 K using nitrogen and helium flow cryostats (Oxford Instruments).

3 Results and Discussion

In this work, the frozen rat tissues of heart, lung, liver and muscle (triceps surae—medial, lateral head of gastrocnemius and soleus muscles) were studied. In the spectra of the tissues after exposing HU model the intense, rather wide EMR signals with the values $g \geq 2.1$ and a characteristic orientation behavior of the resonance field were found at the temperature 77 K. It should be noted that in similar tissues of healthy laboratory rats without any effects or models, such signals are usually do not observe [12]. In the tissues of rats of control group the similar signals were not detected too.

A characteristic feature of all detected signals was the orientation anisotropy of resonance field (H_{res}), i.e., the dependence of signal position on sample orientation in magnetic field of spectrometer. We have studied the angular and temperature dependences of anisotropic signals. Besides broad anisotropic signals, in spectra of some tissues there were also weaker narrow isotropic EPR lines of paramagnetic

centers Fe^{3+}, Cu^{2+} and the signals of free radicals in the vicinity of $g = 2$, typical for biological tissues, which were not the subject of this study.

In rat tissues three types of anisotropic EMR signals were observed (Figs. 1, 2, 3, 4).

The signal of the first type (I) (Figs. 1a, 2a, b) with a g-factor within the range of 1.91–2.36 had the greatest line width $\sim$1100 Oe. Signal was characterized by uniaxial anisotropy (Fig. 2a, b). The angular dependence of the resonance field in the full range of 0°–360° exhibited two maxima and two minima with the period of 180°. Such signals were recorded in lung tissue. Angular H_{res} behavior with uniaxial anisotropy in rat tissues was not detected before.

The signal of the second type (II) (Figs. 1b, 3b) was more narrow with the line width of about 150–300 Oe, g-factor in the range of 2.1–2.4, and an asymmetric line shape. It was characterized by the anisotropy, which was the sum of the axial and cubic contributions. In the angular dependence of H_{res} (0°–360°) four maxima and minima were observed. This type of signal was detected in different tissues: heart, lung, liver and muscle. The signals with similar angular dependences of H_{res} in biological tissues were previously described only in a tissue of mollusk shell and brain of mammals [13] and in ant tissues of head and antennae [14].

To fit the angular dependences of the signals of I- and II-types the equation for ferromagnetic suspended nanoparticles frozen in a magnetic field was used [15]:

$$H_{res}(\theta) = \frac{\omega}{\gamma} - H_{ax}P_2(cos\theta) - H_{cub}\left[1 - \frac{5}{4}\sin^2(2\theta) - \frac{5}{4}\sin^4\theta\sin^2(2\varphi)\right] \quad (1)$$

where H_{ax} and H_{cub} are parameters of axial and cubic field anisotropy, θ and φ are polar and azimuthal angles between magnetization easy-axes and the direction of applied magnetic field in spectrometer. When measuring the angular dependence of the EMR signal, the frozen sample was rotated in horizontal plane, z axis is considered to coincide with the direction of magnetic field H in spectrometer, the angle θ counted from the axis z, and the angle φ was equal to zero.

Simulation and analysis of angular dependence of the resonance field in an arbitrary plane showed that the anisotropy of I-type signal is due to an axial contribution only (for lung tissue the value of H_{ax} was $\sim$320 Oe at the temperature of 150 K), whereas for the II-type signals to the uniaxial anisotropy the cubic contribution was added. It should be noted that the axial anisotropy contribution in

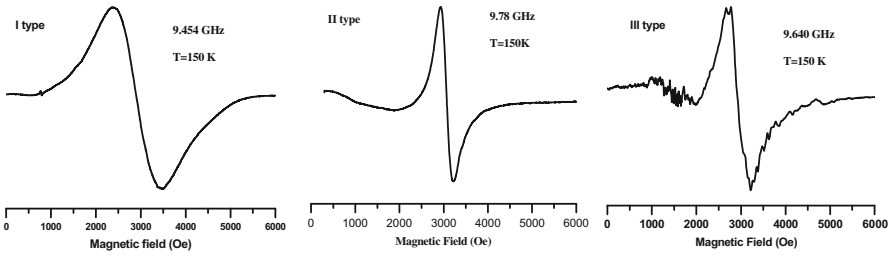

Fig. 1 EMR signals in tissues of rats after HU model exposure: **a** I type signal in lung tissue, **b** II type signal in heart tissue, **c** III type signal in muscle tissue

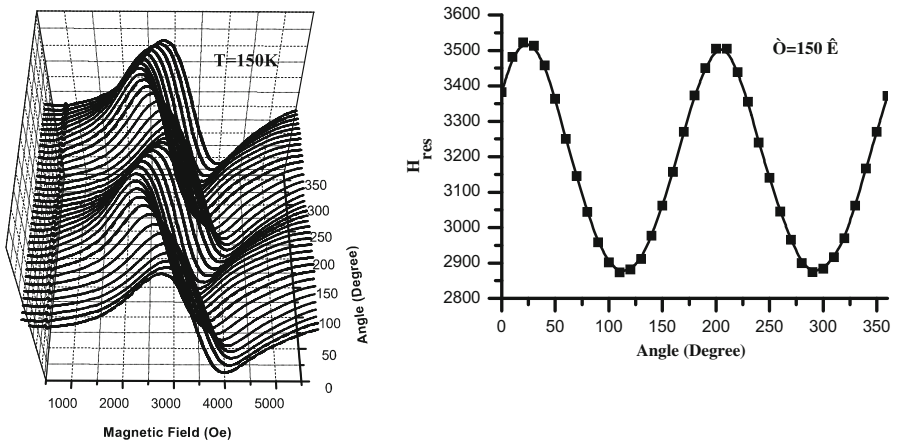

Fig. 2 Angular variation of I type signal: **a** orientation behavior of line, **b** angular dependence of H_{res}

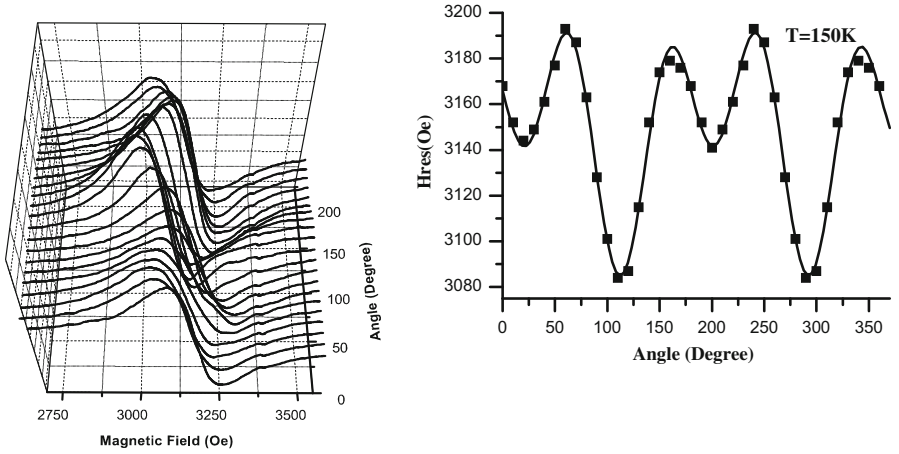

Fig. 3 Angular variation of II type signal: **a** orientation behavior of line, **b** angular dependence of H_{res}

type-II signal was much smaller (for example, at the temperature of 150 K in the sample of heart tissue it was ~40 Oe and cubic contribution was ~60 Oe).

In addition, the signals of third type (III) were recorded, which composed of a rather wide angle-depended EMR line with the width of ~400–700 Oe (Figs. 1c, 4a, b), resonance field H_{res}, depending on the orientation of the sample and sets of "noise like" narrow lines with the width of 20–90 Oe, also depending on the orientation. Such type of spectrum was previously observed only in artificially synthesized samples of ferromagnetic powders, including iron oxides in nonmagnetic matrixes [16–18]. In the samples of biological origin they were detected for the first time. This type of signal was investigated in muscle tissue sample. In angular dependence of this type of signals the broad line had two extreme positions in the field at ~2900 Oe and at ~3200 Oe (at the temperature 150 K). In these

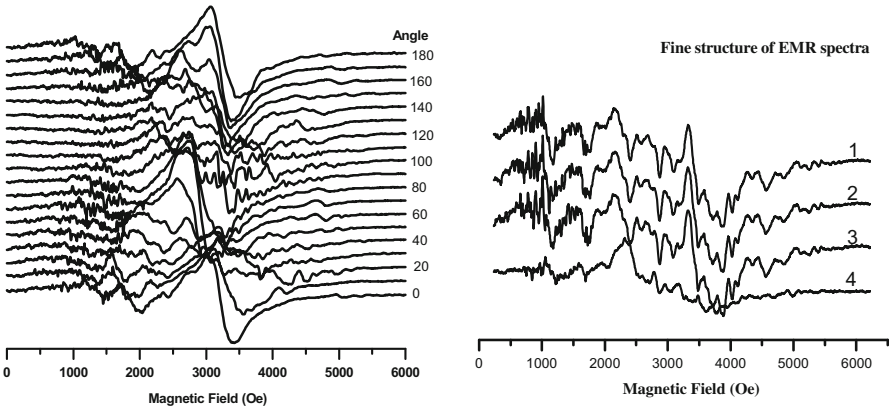

Fig. 4 Angular variation of III type signal **a** orientation behavior of line at 150 K, **b** the example of fine structure of EMR spectra: *1*, *2*, *3* three independent recordings in the same arbitrary orientation at $T = 77$ K, *4* spectrum after the turn of the sample by 5°

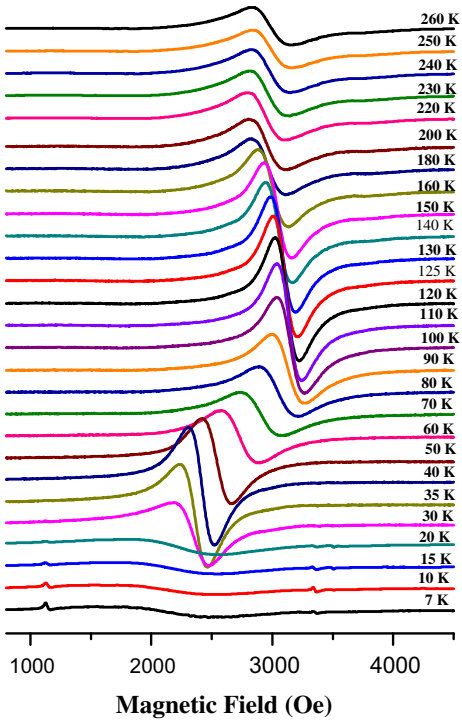

Fig. 5 Temperature behavior of II type signal in heart tissue

orientations the line was the most intensive. In some intermediate orientations the broad EMR line practically disappeared, breaking up into a few smaller lines. Lines of "noise-like" spectrum were recorded in all orientations and their position was also angle-dependent.

Narrow "noise-like" lines, or so-called fine-structure lines (FS) of EMR spectra [16–18]) were observed in the field range from 0 to 6000 Oe, and in the low field part of spectra within the range of approximately (0–2000 Oe), noise-like lines are the most tightly located and have the smallest width of $\sim$20 Oe. The amplitude of the narrow "noise-like" lines at an order exceeds the ordinary instrumental noise of the equipment. One of the character features of this type of signals behavior is complete reproducibility of narrow "noise-like" lines in independent series of recording in the same orientation and at the same temperature (Fig. 4b), but when rotating the sample by a few degrees the spectrum changes dramatically. Such behavior is described in [18]. These narrow lines may be caused by individual single-domain ferrimagnetic magnetite particles of about 50–200 nm in size, which give the individual resonance absorption line. The appearance of the lines of FS in EMR spectra indicates the presence of the dispersed magnetic system of interacting nanoparticles diluted by any non-magnetic material [16–18], in the case of rat tissue sample it may be the organic matter of which the tissue consists.

To understand the nature of recorded signals, we studied the temperature behavior of most intense signal of type II in heart tissue (Fig. 5) and determined dependences of resonance field (H_{res}), line width (ΔH), and the integral intensity on the temperature (Fig. 6a–c) for this signal. Temperature anomalies in these relationships in the temperature range 100–130 K such as—maximum in H_{res} and

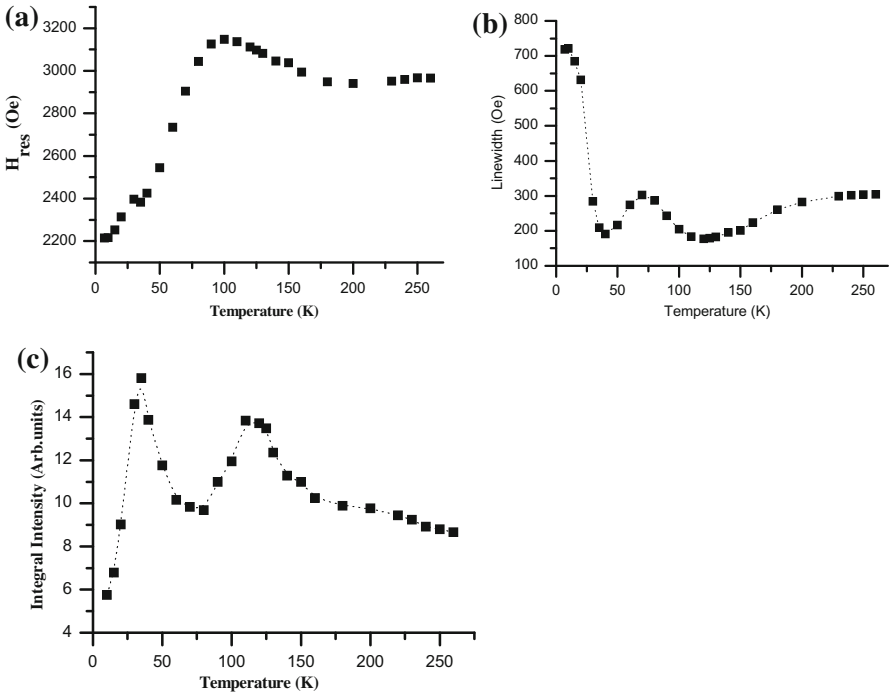

Fig. 6 Temperature variation of **a** resonance field H_{res}, **b** linewidth ΔH, **c** integral intensity for II-type signal

integral intensity, and minimum in ΔH demonstrate Verwey phase transition (VT), characteristic for magnetite [19]. Similar characteristics were previously observed in [20]. The phase transition temperature in a particular sample depends on the degree of crystal non-stoichiometry and the size of the magnetite crystals [21]. The presence of vacancies in magnetite crystalline structure, and the particle size reduction results in a decreasing of the phase transition temperature below the value for a bulk magnetite VT at 124 K [19]. For example, for heart tissue sample the measured inflection point in $H_{res}(T)$ was 100 K. The behavior of parameters $H_{res}(T)$ and $\Delta H(T)$ in high temperature part of dependences correlates with the temperature behavior of the magneto-crystalline anisotropy parameter $K_1(T)$ [22], as described previously in [20]. However, the dependence of the line width (Fig. 6b) is somewhat different from $\Delta H(T)$, given in [20]. In this study, we also found a manifestation of the low-temperature phase transition lower 50 K, character for magnetite and previously found in biogenic magnetite in brain tissue [23]. Above-enumerated features make possible to characterize the source of EMR signal as magnetite, which is confirmed by the temperature dependence of $H_{res}(T)$ for magnetite powders reported in [24].

We have also studied the temperature dependence of the III-type signal above VT (above 100 K). The behavior of $H_{res}(T)$ is similar to Fig. 6a, that confirms, it also belongs to magnetite.

For the II-type signals in the heart tissue the angular dependences at several temperatures of 100, 120, 150 and 180 K were measured (Fig. 7). As a result, it was found that the axial and cubic contributions to anisotropy are changed with the temperature and in the vicinity of VT temperature they change the sign—that seems

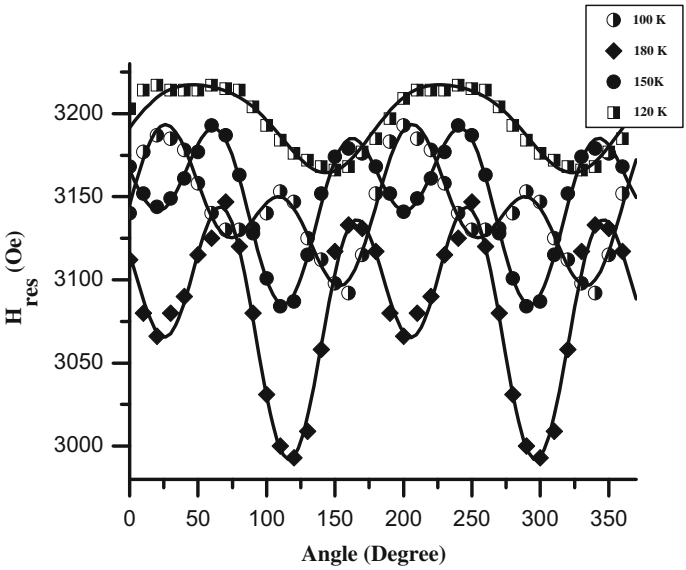

Fig. 7 Angular dependences of H_{res} for II type signal at the temperatures: 100, 120, 150, 180 K and the result of simulation of H_{res} according to formula (Eq. 1)

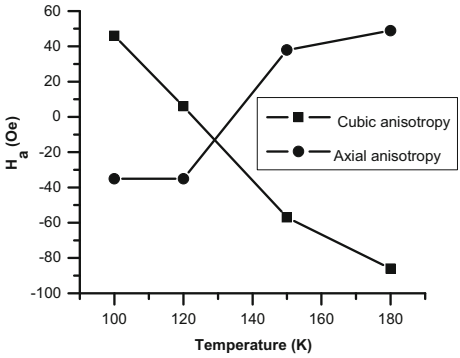

Fig. 8 Temperature variation of parameters H_{ax} and H_{cub}

to reflect the processes near the isotropic point ($\sim$130 K) [22] (Fig. 8). Change of H_{cub} contribution reflects the temperature variation of the magneto-crystalline anisotropy parameter $K_1(T)$ in magnetite [22].

It should be noted that different orientation behavior of the three types of signals represent different forms of accumulation of crystalline iron oxides in tissues. Thus, the behavior of the signal type I, registered in lung tissue, corresponds to the behavior of thin magnetite films [25], the behavior of the signal type II (recorded in the different tissues) the three-dimensional ensemble of nanoparticles of magnetite, a multilayer film of magnetite or bulk-magnetite [26, 27], III-type signals detected in muscle and lung may indicate the presence of regions with a finely dispersed inclusions of magnetite [16–18], that may be connected with the peculiarities of cell structure. As it was established previously [18], "noise-like" spectra are FMR absorption lines due to weakly interacting particles of magnetite. For biological tissue the existence of such areas indicates the inhomogeneous accumulation of iron in the tissues, or probably some local destruction of cells or tissues. Signals similar to III-type signals we also recorded earlier in tumor tissues after radiation and chemotherapy. Their temperature behavior in the high-temperature phase also corresponded to magnetite, and below 90 K, the signal disappeared.

Signal of I type, with axial anisotropy, character to ultrathin ferromagnetic films, was recorded only in lung tissue. Such anisotropy type for signal I may be explained by assuming that the crystal particles of magnetite are mineralized on the surface of lung alveoles, whose structure allows the formation of thin films. Furthermore, the accumulation of particles in the form of thin films is possible in cell membranes, as it is known that the molecules of ferritin, catching the flow of extra iron ions, coming from outside the cell are located on cell membranes and magnetite may be a byproduct of ferritin crystal core growth.

It is known that as the film thickness increases, the contribution of cubic anisotropy is growing too, but the axial anisotropy contribution decreases inversely proportional to film thickness [26]. This situation is typical for signals of type II, and every sample is characterized by its own individual parameters of axial and cubic anisotropy. For signals of type II axial contribution was several times smaller than the axial contribution for I type signal, that indicates a greater thickness of the films

or bulk-magnetite (large pieces of magnetite over 1 μm size). Thus, according to inversely proportional relation of H_{ax} to film thickness [26] parameter 60 Oe may correspond to the thickness ~125 nm and parameter ~320 Oe to the thickness ~7 nm.

Therefore, the different anisotropic behavior of signals, characterizing the spatial distribution of the crystal particles in different tissues may reflect the different scale or degree of heterogeneity of biomineralization, and the peculiarities in structure of tissues and cells of different organs: lung, liver, muscle and heart.

It should be also noticed that described above signals were observed not in all studied tissue samples after the application of HU model. This fact may indicate the different degree of adaptation to short-term microgravity effects in different individual animals. However, 40–50 % of samples of each tissue type demonstrated such orientation depended lines.

The study of tissues by EPR spectroscopy has revealed an abnormal accumulation of aggregated iron form in rat tissues after microgravity simulation, which is not observed in tissues under normal conditions. It may be a consequence of increase in free iron pool in tissues in simulated microgravity conditions, and as a result, a spontaneous biomineralization of magnetite nanocrystals.

It is known [28] that microgravity alters the structure of skeletal muscle and myocardium. Perhaps one of the reasons for the increased free iron pool is the destruction of myoglobin and outcome of iron out of it, as well as the destruction of mitochondria and the outcome of cytochromes, containing heme structures. Consequently, the accumulation of extra iron in crystalline forms such as magnetite nanoparticles may occur. It should be noted also that similar EPR signals, as we found, previously were recorded in blood serum EPR spectra of professional sportsmen undergoing intensive physical exercises [29]; intense physiological processes in their muscles are accompanied by the microdamages of myofibrils.

4 Conclusions

The results obtained in this study indicate the alteration of iron metabolism in rat tissues in simulated microgravity conditions. It was also shown that there is an abnormal accumulation of aggregated forms of iron oxides in rat tissues. The iron storage presents in tissues of lung, heart, liver, and muscle in the form of crystalline structures, particularly in the form of magnetite. The results are of interest for space medicine; they give an opportunity to use highly sensitive EPR spectroscopy technique to study the molecular processes associated with disturbances of iron metabolism in conditions of weightlessness and simulated microgravity.

Acknowledgments The present research by EPR spectroscopy was carried out under the support of Scientific Program of Presidium of RAS 1.26 P during 2015–2016 and rat tissue samples after simulated microgravity model were obtained within the support of Grant RFBR 15-04-05951. V.N. Efimov is also grateful for financial support by the subsidy allocated to Kazan Federal University for the state assignment in the sphere of scientific activities.

References

1. M.G. Tairbekov, *Gravitational Biology of the Cell (Theory and Experiment)* (Moscow Press, Moscow, 1997). **(in Russian)**
2. L.I. Kakurin, V.I. Lobachik, V.M. Mikhailov, YuA Senkevich, Aviat. Space Environ. Med. **47**(10), 1083–1086 (1976)
3. E.R. Morey-Holton, R.K. Globu, J. Appl. Physiol. **92**, 1367–1377 (2002)
4. E.A. Kovalenko, Kosmicheskaya Biologiya i Aviakosmicheskaya Meditsina **11**(4), 3–9 (1977). **(in Russian)**
5. Y. Ohira, T. Wakatsuki, W. Yasui, S. Sugawara, K. Koyanagi, N. Kobayashi, in *Proceedings of Third International Symposium on Space Medicine*, Nagoya, pp. 299–305 (1992)
6. F.W. Booth, C.R. Kirby, Am. J. Physiol. **262**, R329–R332 (1992)
7. A.A. Levina, Z.G. Shishkanova, S.M. Ivanova, T.N. Levina, M.M. Tsibulskaya, O.I. Labetskaya, V.V. Karashtin, G.I. Kozinets, Klinicheskaia Laboratornaia Diagnostika **7**, 3–5 (1998). **(in Russian)**
8. J.L. Kirschvink, D.S. Jones, B.J. MacFadden, *Magnetite Biomineralization and Magnetoreception in Organisms* (Plenum Press, New York, 1985)
9. J.L. Kirschvink, Bioelectromagnetics **10**, 239–260 (1989)
10. E. Mosiniewicz-Szablewska, A. Slawska-Waniewska, K. Świątec, N. Nedelko, J. Galazka-Friedman, A. Friedman, Appl. Magn. Reson. **24**, 429–435 (2003)
11. O. Mykhailyk, G. Török, O. Dudchenko, O. Stavinska, N. Dudchenko, F. Steinberg, J. Magn. Magn. Mater. **272–276**, 2422–2423 (2004)
12. J.I. Azhipa, *Medical-Biological Aspects of Electron Paramagnetic Resonance Applications* (Nauka Press, Moscow, 1983). **(in Russian)**
13. A.B. Brik, Miner. J. (Ukraine) **25**, 16–26 (2003)
14. L.G. Abracado, D.M.S. Esquivel, E. Wajnberg, J. Magn. Magn. Mater. **320**, e204–e206 (2008)
15. H. Li, M.T. Klem, K.B. Sebby, D.J. Singel, M. Young, T. Douglas, Y.U. Idzerda, J. MMM **321**, 175–180 (2009)
16. M.M. Yulikov, O.N. Martyanov, V.F. Yudanov, Appl. Magn. Res. **23**, 105–112 (2002)
17. O.N. Matryanov, S.N. Trukhan, V.F. Yudanov, Appl. Magn. Res. **33**, 57–71 (2008)
18. V.Yu. Petukhov, N.Yu. Panarina, N.R. Khabibullina, E.P. Zheglov, A.A. Mozhanova, Appl. Magn. Reson. **30**, 233–242 (2006)
19. F. Walz, J. Phys. Condens. Matter **14**, R285–R340 (2002)
20. S.V. Yurtaeva, V.N. Efimov, N.I. Silkin, A.A. Rodionov, M.V. Burmistrov, A.V. Panov, A.A. Moroshek, Appl. Magn. Reson. **42**(3), 299–311 (2012)
21. A.R. Muxworthy, E. McClelland, Geophys. J. Int. **140**, 101–114 (2000)
22. R. Řezníček, V. Chlan, H. Štěpánková, P. Novák, M. Maryško, J. Phys. Condens. Matter **24**, 055501 (2012)
23. A.M. Hirt, F. Brem, M. Hanzlik, D. Faivre, J. Geophys. Res. **111**(1–10), B12S06 (2006)
24. M. Hagiwara, K. Nagata, K. Nagata, J. Phys. Soc. Japan **67**(10), 3590–3600 (1998)
25. Z.C. Huang, X.F. Hu, Y.X. Xu, Y. Zhai, Y.B. Xu, J. Wu, H.R. Zhai, J. Appl. Phys. **111**(1–3), 07C108 (2012)
26. L. McGuigan, R.C. Barklie, Phys. Rev. B **77**(1–9), 174424 (2008)
27. L.R. Bickford, Phys. Rev. **78**(4), 449–457 (1950)
28. A.I. Grigoriev, B.S. Shenkman, Skeletal muscle during unloading. Her. Russian Acad. Sci. **78**(4), 337–345 (2008). **(in Russian)**
29. M.I. Ibragimova, A.I. Chushnikov, G.V. Cherepnev, V.Yu. Petukhov, E.P. Zheglov, Biophysics **59**(3), 425–430 (2014)